# Cu 3 C 4 − : A New Sandwich Molecule with Two Revolving C 2 2− Units

**ARTICLE** *in* THE JOURNAL OF PHYSICAL CHEMISTRY A · MARCH 2005

Impact Factor: 2.69 · DOI: 10.1021/jp047384q · Source: PubMed



**4 AUTHORS**, INCLUDING:

Anastassia N Alexandrova
University of California, Los Angeles
**79** PUBLICATIONS **1,981** CITATIONS
SEE PROFILE

Alexander I Boldyrev
Utah State University
**341** PUBLICATIONS **9,936** CITATIONS
SEE PROFILE

Lai-Sheng Wang
Brown University
**434** PUBLICATIONS **18,822** CITATIONS
SEE PROFILE

# $Cu_3C_4^-$: A New Sandwich Molecule with Two Revolving $C_2^{2-}$ Units

**Anastassia N. Alexandrova and Alexander I. Boldyrev***

*Department of Chemistry and Biochemistry, Utah State University, Logan, Utah 84322-0300*

**Hua-Jin Zhai and Lai-Sheng Wang***

*Department of Physics, Washington State University, 2710 University Drive, Richland, Washington 99352, and W. R. Wiley Environmental Molecular Sciences Laboratory, Pacific Northwest National Laboratory, MS K8-88, P.O. Box 999, Richland, Washington 99352*

*Received: June 16, 2004; In Final Form: October 4, 2004*

A combined photoelectron spectroscopy (PES) and ab initio study was carried out on a novel copper carbide cluster in the gas phase: $Cu_3C_4^-$. It was generated in a laser vaporization cluster source and appeared to exhibit enhanced stability among the $Cu_3C_n^-$ series. Its PES spectra were obtained at several photon energies, showing numerous well-resolved bands. Extensive ab initio calculations were performed on $Cu_3C_4^-$, and two isomers were identified: a $C_2$ structure ($^1A$) with a $Cu_3^{3+}$ triangular group sandwiched by two $C_2^{2-}$ units and a linear CuCCCuCCCu structure ($D_{\infty h}$, $^1\Sigma_g^+$). A comparison of ab initio PES spectra with experimental data showed that the sandwich $Cu_3C_4^-$ cluster was solely responsible for the observed spectra and the linear isomer was not present, suggesting that the $C_2$ structure is the global minimum in accordance with CCSD(T)/6-311+G* predictions. Interestingly, a relatively low barrier (0.4−0.6 kcal/mol) was found for the internal rotation of the $C_2^{2-}$ units in the sandwich $Cu_3C_4^-$. To test different levels of theory in describing the $Cu_mC_n^-$ systems and lay foundations for the validity of the theoretical methods, extensive calculations at a variety of levels were also carried out on a simpler copper carbide species $CuC_2^-$, where two isomers were found to be close in energy: a linear one ($C_{\infty v}$, $^1\Sigma^+$) and a triangular one ($C_{2v}$, $^1A_1$). The calculated electronic transitions for $CuC_2^-$ were also compared with the PES data, in which both isomers were present.

## 1. Introduction

Carbides are compounds formed by carbon and elements with similar or lower electronegativity, and they have many important applications in technology.[1−4] Carbides of the highly electropositive metals are saltlike, containing distinct $C^{4-}$, $C_2^{2-}$, or $C_3^{4-}$ anions that release $CH_4$, $C_2H_2$, or $C_3H_4$ hydrocarbons, respectively, upon reaction with water. Carbide clusters have attracted a lot of attention from both theoreticians and experimentalists,[5−27] in particular, after the discovery of the "met-cars", which consist of eight early-transition-metal atoms and six $C_2$ units.[28−34] Bulk copper carbide contains $C_2$ acetylenic units. However, there have been relatively few studies on copper carbide clusters.[35,36] However, cyclic $Cu_n$ structural motifs have been previously reported to be a building block of various organic and inorganic systems.[37−53] In particular, the triangular motif $Cu_3$ has been observed within organic molecules and complexes containing various ligands and bridging groups.[38−48] Interestingly, Lo and co-workers reported the existence of a copper rectangular unit containing an oscillating $C_2^{2-}$ unit inside the $[Cu_4(\mu\text{-dppm})_4(\mu\text{-}\eta^1,\eta^2\text{-}C_2\text{-})]^{2+}$ cation,[37] which was the first observation of a revolving $C_2$ group. Therefore, copper carbide clusters comprising the $Cu_3$ motif and decorated with $C_2$ units may represent chemical species with interesting structural and electronic properties and novel chemical bonding.

The current study is a continuation of our research on the electronic structure and chemical bonding of metal carbide clusters using photoelectron spectroscopy (PES).[11,13−22] We report a combined PES and ab initio study of two copper carbide clusters, $CuC_2^-$ and $Cu_3C_4^-$, that were generated using a laser vaporization cluster beam source. PES spectra were measured at three photon energies (355, 266, and 193 nm), and numerous well-resolved bands were revealed. The experimental PES features were successfully assigned to electron detachment transitions from their lowest-energy structures based on extensive ab initio calculations. Two low-lying isomers were identified for $Cu_3C_4^-$: a unique sandwich structure ($C_2$, $^1A$), containing a $Cu_3^{3+}$ triangular group and two $C_2^{2-}$ units and a linear structure ($D_{\infty h}$, $^1\Sigma_g^+$) in which two $C_2$ units were separated by the Cu atoms. The ab initio photoelectron spectrum of the sandwich $Cu_3C_4^-$ cluster was found to be in better agreement with the experiment, suggesting that it might be the more stable structure. Moreover, a relatively low barrier (0.4−0.6 kcal/mol) was found for the internal rotation of the $C_2^{2-}$ units in the $Cu_3C_4^-$ sandwich. To test different levels of theories in describing the $Cu_mC_n^-$ systems and lay foundations for the theoretical methods, we also carried out extensive calculations on the simplest $Cu_mC_n^-$ species, $CuC_2^-$, for which the calculations were also compared with the PES data.

## 2. Experimental Method

The experiments were carried out using a magnetic-bottle-type PES apparatus equipped with a laser vaporization supersonic cluster source. A detailed description of the experimental techniques can be found elsewhere.[54] Briefly, the $CuC_2^-$ and $Cu_3Cu_4^-$ anions were produced by laser vaporization of a Cu/C mixed target (∼10% C in molar ratio) in the presence of a

* Corresponding authors. E-mail: boldyrev@cc.usu.edu; ls.wang@pnl.gov.

10.1021/jp047384q CCC: $30.25 
Published on Web 01/27/2005

helium carrier gas. Various $Cu_mC_n^-$ clusters were generated and mass analyzed using a time-of-flight mass spectrometer. The $CuC_2^-$ and $Cu_3Cu_4^-$ species of interest were each mass selected and decelerated before being photodetached. Three detachment photon energies were used in the current study: 355 nm (3.496 eV), 266 nm (4.661 eV), and 193 nm (6.424 eV). Photoelectrons were collected at nearly 100% efficiency by the magnetic bottle and analyzed in a 3.5-m-long electron flight tube. The photoelectron spectra were calibrated using the known spectrum of $Rh^-$, and the energy resolution of the apparatus was $\Delta Ek/Ek \approx$ 2.5%, that is, ~25 meV for 1-eV electrons.

## 3. Computational Methods

We first characterized the smaller $CuC_2^-$ cluster using several different levels of theory. The initial search for the global minimum of $CuC_2^-$ was carried out using the hybrid method, including a mixture of Hartree−Fock exchange with density functional exchange−correlation potentials (B3LYP)[55−57] and the polarized split-valence basis set (6-311+G*).[58−60] Optimized geometries and vibrational frequencies were refined using the coupled-cluster method including single and double excitations and with triple excitations treated noniteratively [CCSD(T)].[61−63] Two different basis sets were used at this level of theory: 6-311+G* and for the pseudopotential calculations we used the LANL2DZ[64−66] basis set, extended by additional s ($\alpha = 0.1533$), p ($\alpha = 0.1146$), and d ($\alpha = 0.1320$) functions on C and s ($\alpha =$ 0.3960), p ($\alpha = 0.2400$), and d ($\alpha = 0.3102$) functions on Cu. For the $Cu_3C_4^-$ cluster, we also tested the second-order Mólller−Plesset perturbation theory method MP2[67−69] and the CCSD-(T) with the 6-311+G* basis set.

Geometries and vibrational frequencies of the $Cu_3C_4^-$ alternative structures were calculated using the B3LYP/6-311+G* level of theory. The molecular parameters of the lowest-energy isomers were then recalculated using the MP2/6-311+G* and the B3LYP/LANL2DZ(spd) methods. Energies of the lowest isomers were also refined at the CCSD(T)/6-311+G* and MP2full/6-311+G(2df) levels.

Theoretical vertical detachment energies (VDE) of the $CuC_2^-$ cluster were obtained at both the CCSD(T) and the time-dependent density-functional (B3LYP) levels of theory with the 6-311+G(2df) basis set. VDEs of the $Cu_3C_4^-$ lowest-energy isomers were calculated using only the time-dependent density functional (TD-B3LYP) method[70,71] with the 6-311+G(2df) basis set. In this approach, the vertical electron detachment energies were calculated as a sum of the lowest transitions from the singlet state of the anion into the final lowest doublet state of the neutral species (at the B3LYP level of theory) and the vertical excitation energies in the neutral species (at the TD-B3LYP level). Natural population analysis (NPA)[72] at the B3LYP/6-311+G* level was run for the verification of the nature of the chemical bonding of the low-energy isomers. Molecular orbitals were calculated at the HF/6-311+G* level of theory.

All B3LYP, CCSD(T), MP2, CASSCF, and NPA calculations were performed using the Gaussian 98 program.[73] TD-B3LYP calculations were done using the Gaussian 03 package.[74] Molecular orbital pictures were made using the MOLDEN3.4 program.[75]

## 4. Experimental Results

**4.1. Mass Spectrum of $Cu_mC_n^-$.** A variety of $Cu_mC_n^-$ cluster anions were generated from the laser vaporization supersonic cluster source.[54] A typical time-of-flight mass spectrum is shown in Figure 1. The mass spectrum was easily assigned peak-by-peak on the basis of the characteristic isotope pattern of Cu (69.17% $^{63}Cu$ and 30.83% $^{65}Cu$). As shown in Figure 1, two series of copper carbide clusters, $CuC_n^-$ ($n = 7-14$) and $Cu_2C_n^-$ ($n = 3-9$), were identified. The $^{63}Cu^{65}CuC_n^-$ mass peak is only 1 amu less than the $^{63}Cu^{63}Cu^{63}CuC_{n-5}^-$ mass peak, so the former is partially overlapped with the latter and appears in the mass spectrum as a shoulder, which broadened the peak width of the latter as observed. $Cu_3C_4^-$ appeared to be the dominant species in the $Cu_3C_n^-$ series, indicating its somewhat enhanced stability. This observation drew our attention. The $Cu_3C_4^-$ mass distribution, labeled with vertical bars in Figure 1, was confirmed by comparing with the simulated isotope pattern (inset, Figure 1). Note that the 237 amu peak of $Cu_3C_4^-$ contained a partial contribution from $^{63}Cu^{65}CuC_9^-$ (236 amu). However, the 239, 241, and 243 amu isotope peaks of $Cu_3C_4^-$ should be pure. Our current photodetachment experiments on $Cu_3C_4^-$ were therefore conducted with both the 239 and 241 amu peaks, and identical PES spectra were obtained. (See below.)

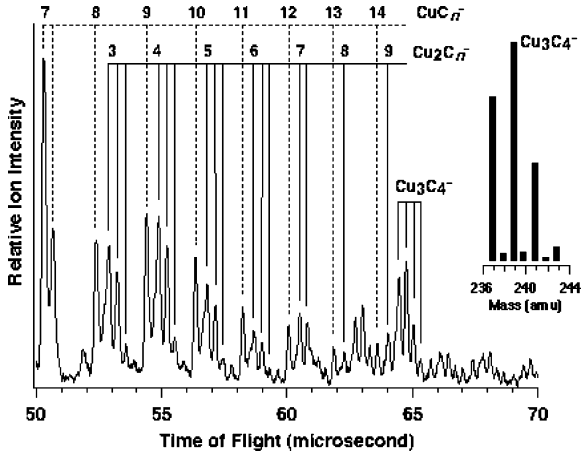


**Figure 1.** Typical time-of-flight mass spectrum of $Cu_mC_n^-$ clusters from the laser vaporization supersonic cluster source. Mass peaks for $CuC_n^-$ ($n = 7-14$), $Cu_2C_n^-$ ($n = 3-9$), and $Cu_3C_4^-$ were assigned on the basis of the isotope distributions. Note that the $Cu_3C_4^-$ cluster appeared to be especially abundant among the $Cu_3C_n^-$ series. The inset shows the simulated isotope distribution of $Cu_3C_4^-$.

**4.2. Photoelectron Spectra of $CuC_2^-$.** The $CuC_2^-$ species (not shown in Figure 1) was the smallest and weakest among all of the $Cu_mC_n^-$ clusters produced from our source. Its PES spectra at the three photon energies are shown in Figure 2. These spectra turned out to be dominated by features from atomic $Cu^-$, as labeled by the asterisks. The $Cu^-$ signals were due to a two-photon process as a result of photofragmentation, $CuC_2^- + h\nu \rightarrow Cu^- + C_2$, followed by the photodetachment of $Cu^-$ by a second photon. We noted that the relative intensities of the three peaks of $Cu^-$ seemed to be different from those of free $Cu^-$, in particular, at 355 nm, where the first peak at 1.23 eV due to the removal of a 4s electron is stronger than the two higher-binding-energy peaks due to the removal of a 3d electron.[76] This intensity variation was not due to any instrumental artifact and might be the result of certain alignment effect in the nascent $Cu^-$ anion. We also observed weak $C_2^-$ signals around 3.27 eV[77,78] due to another fragmentation channel: $CuC_2^- + h\nu \rightarrow Cu + C_2^-$. The observation of facile $CuC_2^-$ photofragmentation suggests that it is a weakly bonded species between Cu and $C_2$, consistent with its very weak intensity from the cluster source.

The sharp peak at 2.26 eV (X) is due to the ground-state transition of $CuC_2^-$. This peak is as sharp as the $Cu^-$ atomic transitions without a vibrational progression, suggesting the removal of a nonbonding electron and that there is no geometry

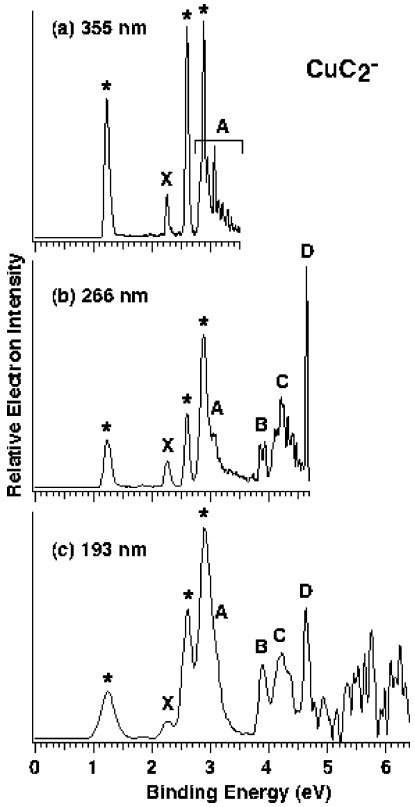


**Figure 2.** Photoelectron spectra of $CuC_2^-$ at (a) 355 nm (3.496 eV), (b) 266 nm (4.661 eV), and (c) 193 nm (6.424 eV). The features labeled with asterisks (∗) are due to $Cu^-$ from photofragmentation.

**TABLE 1. Observed Adiabatic (ADE) and Vertical (VDE) Detachment Energies from the Photoelectron Spectra of $CuC_2^-$**

| observed feature | VDE (eV)[a] |
|---|---|
| X | 2.26(3)[b] |
| A | 2.8−3.4 |
| B | 3.88(5) |
| C | 4.22(5) |
| D | 4.63(2) |

[a] Numbers in parentheses represent the experimental uncertainties in the last digit. [b] ADE = 2.26(3) eV.

change between the ground state of $CuC_2^-$ and that of neutral $CuC_2$. At the higher-binding-energy side of the 355-nm spectrum (Figure 2a), more features (A) were observed between 2.8 and 3.4 eV, most likely because of vibrational excitations in a single electronic transition. The overlap of the A band with a strong $Cu^-$ peak as well as a small contribution from the $C_2^-$ fragmentation product around 3.27 eV made it difficult for us to evaluate adiabatic (ADE) and vertical (VDE) detachment energies for this band as well as the vibrational information. The 266-nm spectrum (Figure 2b) further revealed three bands for $CuC_2^-$: B and C with likely vibrational structures and a sharp peak D at 4.63 eV. At 193 nm, no well-defined features could be identified beyond 5.0 eV (Figure 2c), probably because of the poor statistics. All of the observed ADEs and VDEs are collected in Table 1.

**4.3. Photoelectron Spectra of $Cu_3C_4^-$.** The PES spectra of $Cu_3C_4^-$ are shown in Figure 3. Because of potential mass overlaps with other stoichiometry, photodetachment experiments were conducted with both the 239 and 241 amu isotope peaks (Figure 1), which yielded identical PES spectra. The 266-nm spectrum (Figure 3a) revealed four well-resolved bands (X, A, B, and C). The ground-state transition X was rather weak and was vibrationally resolved at 355 nm (inset in Figure 3a) with a short vibrational progression and a spacing of 440 ± 50 $cm^{-1}$. The 0−0 transition at 3.07 ± 0.02 eV defines the ground-state ADE and VDE of $Cu_3C_4^-$, which also represents the electron affinity of the $Cu_3C_4$ neutral. The VDEs for features A, B, and C were measured to be 3.73, 3.97, and 4.32 eV, respectively. Feature A was much stronger than feature B, whereas feature C appeared to be the most intense in the 266-nm spectrum. In contrast to the spectra of $CuC_2^-$, no observable photofragmentation was observed in the spectra of $Cu_3C_4^-$ due to either $Cu_3^-$ or $C_2^-$. The former would yield a band around 2.37 eV,[79] whereas the latter would yield signals around 3.37 eV (recite the two refs on $C_2^-$ here).

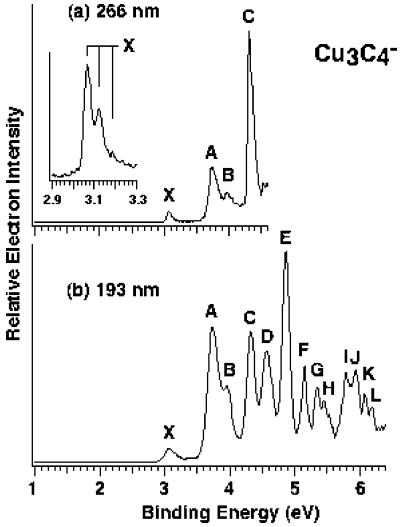


**Figure 3.** Photoelectron spectra of $Cu_3C_4^-$ at (a) 266 nm and (b) 193 nm. The inset in spectrum shows the vibrational progression of ground-state transition X at 355 nm. The vertical bars represent the resolved vibrational structures.

**TABLE 2. Observed Adiabatic and Vertical Detachment Energies and Vibrational Frequencies from the Photoelectron Spectra of $Cu_3C_4^-$**

| observed feature | VDE (eV)[a] |
|---|---|
| X[b,c] | 3.07(2)[b] |
| A | 3.73(3) |
| B | 3.97(3) |
| C | 4.32(2) |
| D | 4.58(3) |
| E | 4.87(3) |
| F | 5.16(3) |
| G | 5.35(3) |
| H | 5.46(3) |
| I | 5.80(3) |
| J | 5.94(3) |
| K | 6.08(3) |
| L | 6.20(3) |

[a] Numbers in parentheses represent the experimental uncertainties in the last digits. [b] ADE = 3.07(2) eV [c] The ground-state vibrational frequency of the neutral $Cu_3C_4$ was measured to be 440 ± 50 $cm^{-1}$ from the resolved vibrational structures (Figure 2).

In the 193-nm spectrum (Figure 3b), feature X remained the weakest and feature A remained much stronger than feature B, but the relative intensity of feature C was remarkably reduced. Nine more bands (D−L) were clearly identified and labeled at higher binding energies. The ADEs and VDEs for all of the PES features are collected in Table 2.

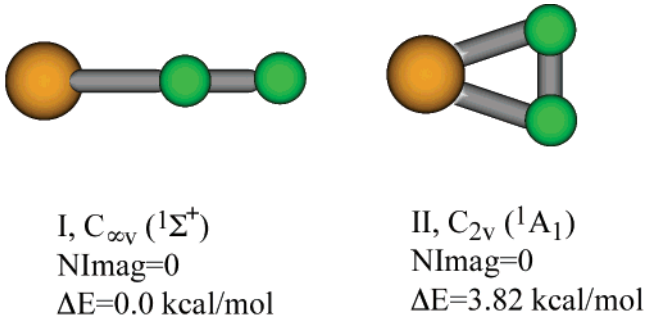


**Figure 4.** Lowest-energy structures of the $CuC_2^-$ cluster at the B3LYP/6-311+G* level of theory.

## 5. Theoretical Results

**5.1. $CuC_2^-$.** First, we performed an extensive search for the most stable structures of $CuC_2^-$ using the B3LYP/6-311+G* level of theory. The two most stable isomers are shown in Figure 4 and their molecular parameters are summarized in Tables S1 and S2 (Supporting Information). At the B3LYP/6-311+G* level of theory, the global minimum structure is the linear $C_{\infty v}$ ($^1\Sigma^+$) (Figure 4) with electronic configuration $1\sigma^2 1\pi^4 1\delta^4 2\sigma^2 3\sigma^2 4\sigma^2 2\pi^4$. The second triangular $C_{2v}$ ($^1A_1$) isomer with a $1a_1^2 1b_2^2 1b_1^2 2a_1^2 1a_2^2 2b_2^2 3a_1^2 4a_1^2 2b_1^2 5a_1^2$ electronic configuration is just 3.8 kcal/mol higher in energy at this level of theory. The barrier for the $CuC_2^-$ ($C_{2v}$, $^1A_1$) → $CuC_2^-$ ($C_{\infty v}$, $^1\Sigma^+$) intramolecular rearrangement is only 1.3 kcal/mol at the B3LYP/6-311+G* level of theory, and it is almost vanished after the zero-point energy (ZPE) correction.

At the MP2/6-311+G* level of theory, we found that both the linear and triangular structures are minima with the triangular structure ($C_{2v}$, $^1A_1$) being more stable than the linear one ($C_{\infty v}$, $^1\Sigma^+$) by 2.5 kcal/mol (Tables S1 and S2). Optimized geometric parameters and harmonic vibrational frequencies agree reasonably well with the corresponding B3LYP/6-311+G* values.

When the CCSD(T)/6-311+G* level of theory was employed for geometry optimization, the $C_{2v}$ structure was found to be the global minimum on the potential energy surface, whereas the linear isomer is 0.9 kcal/mol above the global minimum. The barrier for $CuC_2^-$ ($C_{2v}$, $^1A_1$) → $CuC_2^-$ ($C_{\infty v}$, $^1\Sigma^+$) is only 1.8 kcal/mol at the CCSD(T)/6-311+G* level of theory, and it is 1.4 kcal/mol after the ZPE correction. The use of LANL2DZ(spd) makes the triangular isomer 5.6 kcal/mol more stable than the linear one. To test further the relative stability of the two lowest structures, we used the CCSD(T)/6-311+G(2df)//CCSD(T)/6-311+G* method, which predicted the triangular structure to be 0.7 kcal/mol higher in energy than the linear one. Clearly, it is difficult to judge the global minimum structure of $CuC_2^-$ solely on the basis of quantum chemical calculations, which showed that the linear and triangular structures are very close in energy. From comparisons of ab initio and experimental photoelectron spectra, we found that both isomers might be present in the molecular beam and may have contributed to the photoelectron spectra. Indeed, as will be shown in section VI, the experimental spectra can be interpreted only if both isomers are taken into consideration.

As one may see from Tables S1 and S2, optimized geometric parameters and harmonic frequencies for $CuC_2^-$ obtained at different levels of theory are in reasonable agreement. This fact is very important for the subsequent investigation of the larger system (i.e., $Cu_3C_4^-$) because some of the high-level calculations are beyond our current computational resources.

**5.2. $Cu_3C_4^-$.** The initial extensive search for the global minimum structure of the $Cu_3C_4^-$ cluster was carried out at the B3LYP/6-311+G* level of theory. Several optimized structures are shown in Figure 5. The molecular parameters to the two lowest-energy isomers (I and II) are summarized in Tables 3 and 4, respectively. At the B3LYP/6-311+G* level, lowest-energy isomer I has a linear $D_{\infty h}$ ($^1\Sigma_g^+$) structure with an electronic configuration of $1\sigma_g^2 1\sigma_u^2 2\sigma_g^2 2\sigma_u^2 3\sigma_g^2 1\pi_g^4 1\pi_u^4 1\delta_g^4 1\delta_u^4 3\sigma_u^2 4\sigma_g^2 2\pi_g^4 4\sigma_u^2 2\delta_g^4 2\pi_u^4 5\sigma_g^2 3\pi_g^4$. The second $C_2$ ($^1A$) sandwich-type structure II is 6.50 kcal/mol higher in energy at the B3LYP/6-311+G* level of theory with an electronic configuration of $1a^2 1b^2 2a^2 2b^2 3a^2 3b^2 4a^2 4b^2 5a^2 5b^2 6a^2 6b^2 7a^2 7b^2 8a^2 9a^2 8b^2 9b^2 10a^2 11a^2 10b^2 12a^2 11b^2 12b^2 13a^2$. Alternative sandwich structure V ($D_{3h}$, $^1A_1'$, Figure 5) with two $C_2^{2-}$ groups oriented perpendicular to the triangular $Cu_3$ was found to be a fourth-order saddle point and substantially higher in energy. Geometries and energies of the lowest-energy species were recalculated at the MP2/6-311+G* level of theory. Optimized geometries and harmonic frequencies were found to be in reasonable agreement with the B3LYP/6-311+G* results. However, the sandwich structure is now more stable than the linear one by 12.8 kcal/mol. At the CCSD(T)/6-311+G*//B3LYP/6-311+G* level of the theory, sandwich structure II was also found to be more stable, having an energy 16.0 kcal/mol lower than the linear isomer. We also will rely on comparisons with the experimental data to determine which structure is more stable.

Structures III and IV in Figure 5, with the two $C_2$ units perpendicular and parallel to each other, respectively, were shown to be first-order saddle points and represent transition states of the internal $C_2$ rotation in sandwich structure II. We calculated a potential energy curve of this internal rotation (Figure 6) at the B3LYP/6-311+G* level of theory as a function of the dihedral angle $\phi$ between two $C_2$ groups. Minimum structure II appeared four times corresponding to $\phi = 60$, 120, 240, and 300°. (Only the first two structures are shown in Figure 6.) Transition-state structure III ($C_s$, $^1A'$) with $\phi = 90$ and 270° was found to be only 0.6 kcal/mol above the minimum structures, whereas transition-state structure IV ($C_{2v}$, $^1A_1$) with $\phi = 0$ and 180° was found to be 0.4 kcal/mol above the minimum structures. Even though our calculated values for the barriers are certainly rather crude, our results suggest almost free rotations of the $C_2$ groups in the sandwich structure. This conclusion is similar to what was previously observed for the $[Cu_4(\mu\text{-dppm})_4(\mu\text{-}\eta^1,\eta^2\text{-}C_2\text{-})]^{2+}$ cation.[37]

## 6. Interpretation of the PES Spectra and Comparison with Theoretical Results

**6.1. $CuC_2^-$.** Table 5 shows the calculated VDEs of the two low-lying isomers of $CuC_2^-$. Because both isomers are closed-shell systems, their calculated spectra are relatively simple: each fully occupied MO gives rise to one detachment transition if one ignores the spin−orbit splitting. First, we note that we got reasonable agreement between the two levels of theory for the calculated detachment energies for both isomers. Comparing the calculated VDEs with the experimental data (Figure 2 and Table 1), we can easily assign the lowest detachment feature observed for $CuC_2^-$ (X) to triangular isomer II. The calculated VDE (2.28 eV) from the HOMO ($5a_1$) of the $C_{2v}$ isomer is in excellent agreement with the experimental value of $2.26 \pm 0.03$ eV. This MO is largely a nonbonding orbital consisting of Cu 4s and C 2p (Figure S2), in agreement with the sharp PES band, which contains little vibrational activity (Figure 2).

Even though band A was overlapped with a strong peak from $Cu^-$, it could be seen that it contained several peaks in the range from 2.8 to 3.4 eV. The detachment from HOMO-1 of isomer

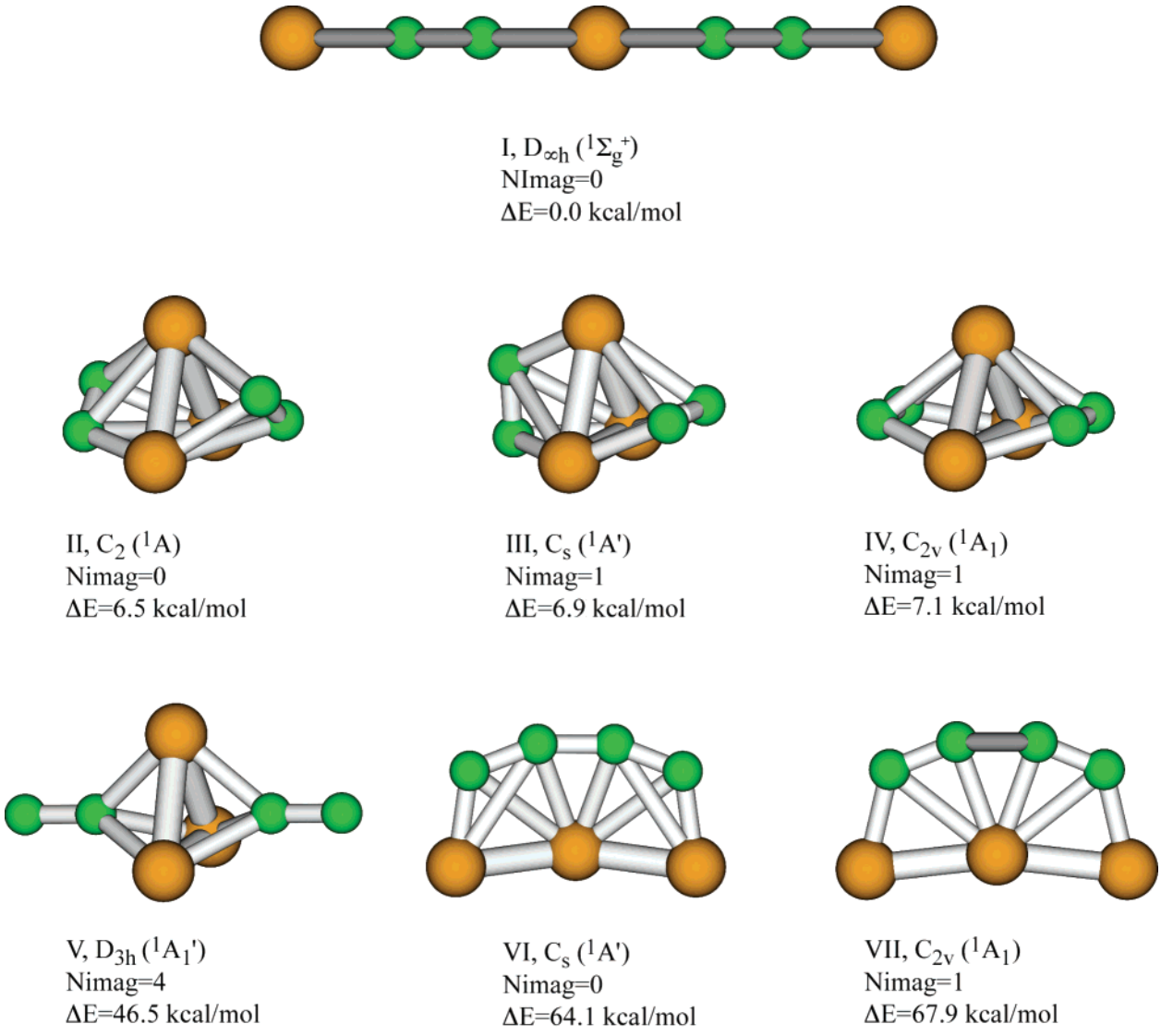


**Figure 5.** Alternative structures of the $Cu_3C_4^-$ cluster at the B3LYP/6-311+G* level of theory.

II should occur in this energy range. The calculated VDE for this detachment channel is 2.92 eV at CCSD(T) and 2.63 eV at TD-B3LYP (Table 5). Interestingly, the VDEs of the first two detachment channels from linear isomer I also fall in this energy range. The spectral pattern of band A strongly suggested the contributions from this isomer. The third detachment channel from the linear isomer was calculated at 3.74 eV, which should correspond to band B. Band C at 4.22 eV is in good agreement with the detachment from HOMO-2 of isomer II with a calculated VDE of 4.11 eV. The next detachment channel for isomer II was calculated at 5.39 eV. Thus, strong band D is likely due to detachment of the linear isomer from HOMO-3, which was not calculated.

Therefore, the calculated VDEs for isomers I and II allowed a reasonable account of the observed PES spectra of $CuC_2^-$, strongly suggesting the coexistence of both isomers from our source. The relative spectral intensities indicated that both isomers were present in almost equal proportion, implying that the two isomers are nearly degenerate energetically, as predicted theoretically. This is an interesting result, indicating that there is not a strong directional preference for the bonding between Cu and $C_2$. This is consistent with their ionic bonding character.

**6.2. $Cu_3C_4^-$.** Theoretical VDEs of the two lowest-energy isomers of the $Cu_3C_4^-$ cluster calculated at the TD B3LYP/6-311+G(2df) level of theory are given in Table 6. The first VDEs calculated for both the $D_{\infty h}$ and the sandwich $C_2$ structures are similar and are in good agreement with the first VDE (band X) observed experimentally at 3.07 eV (Figure 3 and Table 2). Thus, the first band cannot be used to distinguish the presence of either or both isomers. However, the VDEs of the second detachment channel for the two isomers are very different (Table 6). The calculated VDE for the second detachment channel for the linear isomer was 3.32 eV, which disagrees with the experimental VDE of 3.73 eV (Figure 3 and Table 2). However, the calculated VDE for the second detachment channel for the sandwich $C_2$ isomer was 3.73 eV, which is in quantitative agreement with the experimental measurement. In fact, the whole spectral pattern calculated for the sandwich isomer is in excellent agreement with the observed PES spectra. This observation clearly eliminated the presence of the linear isomer in the experiment and confirmed that the PES spectra of $Cu_3C_4^-$ observed experimentally were entirely due to the sandwich isomer. In other words, the linear isomer was not present in the experiment with detectable abundance.

The ground-state transition of $Cu_3C_4^-$ was vibrationally resolved, yielding a vibrational frequency of 440 ± 50 $cm^{-1}$ for neutral $Cu_3C_4$. We note that the calculated frequency for the totally symmetric $\nu_2$ (a) mode for $Cu_3C_4^-$ is about 460 $cm^{-1}$

**TABLE 3. Calculated Molecular Properties of the $Cu_3C_4^-$ $D_{\infty h}(^1\Sigma_g^+)$ Linear Isomer**

| | B3LYP/6-311+G* | | | | B3LYP/LANL2DZ(spd) | | | | MP2/6-311+G* | | | |
|---|---|---|---|---|---|---|---|---|---|---|---|---|
| $E_{tot}$, au | −5073.906646[a] | | | | −740.780126 | | | | −5069.815117[b] | | | |
| Nimag | 0 | | | | 0 | | | | *c* | | | |
| | | *x* | *y* | *z* | | *x* | *y* | *z* | | *x* | *Y* | *z* |
| | Cu | 0.000 | 0.000 | 4.945 | Cu | 0.000 | 0.000 | 4.987 | Cu | 0.000 | 0.000 | 4.872 |
| | Cu | 0.000 | 0.000 | 0.000 | Cu | 0.000 | 0.000 | 0.000 | Cu | 0.000 | 0.000 | 0.000 |
| | Cu | 0.000 | 0.000 | −4.945 | Cu | 0.000 | 0.000 | −4.987 | Cu | 0.000 | 0.000 | −4.872 |
| geometry, Å | C | 0.000 | 0.000 | 3.131 | C | 0.000 | 0.000 | 3.161 | C | 0.000 | 0.000 | 3.096 |
| | C | 0.000 | 0.000 | 1.889 | C | 0.000 | 0.000 | −3.161 | C | 0.000 | 0.000 | 1.836 |
| | C | 0.000 | 0.000 | −1.889 | C | 0.000 | 0.000 | 1.897 | C | 0.000 | 0.000 | −1.836 |
| | C | 0.000 | 0.000 | −3.131 | C | 0.000 | 0.000 | −1.897 | C | 0.000 | 0.000 | −3.096 |
| | $\omega_1(\sigma_g) = 2033$ | | | | $\omega_1(\sigma_g) = 2017$ | | | | *c* | | | |
| | $\omega_2(\sigma_g) = 630$ | | | | $\omega_2(\sigma_g) = 629$ | | | | *c* | | | |
| | $\omega_3(\sigma_g) = 166$ | | | | $\omega_3(\sigma_g) = 164$ | | | | *c* | | | |
| | $\omega_4(\sigma_u) = 2021$ | | | | $\omega_4(\sigma_u) = 2006$ | | | | *c* | | | |
| | $\omega_5(\sigma_u) = 639$ | | | | $\omega_5(\sigma_u) = 646$ | | | | *c* | | | |
| frequencies, $cm^{-1}$ | $\omega_6(\sigma_u) = 288$ | | | | $\omega_6(\sigma_u) = 289$ | | | | *c* | | | |
| | $\omega_7(\pi_g) = 278$ | | | | $\omega_7(\pi_g) = 264$ | | | | *c* | | | |
| | $\omega_8(\pi_g) = 85$ | | | | $\omega_8(\pi_g) = 87$ | | | | *c* | | | |
| | $\omega_9(\pi_u) = 342$ | | | | $\omega_9(\pi_u) = 331$ | | | | *c* | | | |
| | $\omega_{10}(\pi_u) = 153$ | | | | $\omega_{10}(\pi_u) = 149$ | | | | *c* | | | |
| | $\omega_{11}(\pi_u) = 11$ | | | | $\omega_{11}(\pi_u) = 24$ | | | | *c* | | | |

[a] At the CCSD(T)/6-311+G* level of theory, the total energy is −5069.699920. [b] At the MP2full/6-311+G(2df) level of theory, the total energy is −5071.762456. [c] Molecular property was not calculated at this level of theory.

**TABLE 4. Calculated Molecular Properties of the $Cu_3C_4^-$ $C_2(^1A)$ Sandwich Isomer**

| | B3LYP/6-311+G* | | | | B3LYP/LANL2DZ | | | | MP2/6-311+G* | | | |
|---|---|---|---|---|---|---|---|---|---|---|---|---|
| $E_{tot}$, au | −5073.896288[a] | | | | −740.764230 | | | | −5067.905790[b] | | | |
| Nimag | 0 | | | | 0 | | | | *c* | | | |
| | | *x* | *y* | *z* | | *x* | *y* | *z* | | *x* | *Y* | *z* |
| | Cu | 0.000 | 0.000 | 1.353 | Cu | 0.000 | 0.000 | 1.320 | Cu | 0.000 | 0.000 | 1.322 |
| | Cu | −1.272 | 0.5423 | −0.670 | Cu | 0.000 | 1.553 | −0.603 | Cu | −1.314 | 0.262 | −0.666 |
| | Cu | 1.272 | −0. 542 | −0.670 | Cu | 0.000 | −1.553 | −0. 603 | Cu | 1.314 | −0.262 | −0.666 |
| geometry, Å | C | 0.984 | −1.372 | −0.328 | C | 1.670 | −0.592 | 0.056 | C | 1.126 | 1.490 | 0.333 |
| | C | 0.000 | 1.880 | 0.298 | C | 1.767 | 0.638 | −0.334 | C | 0.000 | 1.595 | −0.311 |
| | C | −0.984 | 1.372 | −0.328 | C | −1.670 | 0.592 | 0.056 | C | −1.126 | −1.490 | 0.333 |
| | C | 0.000 | −1.880 | 0.298 | C | −1.767 | −0.638 | −0.334 | C | 0.000 | −1.595 | −0.311 |
| | $\omega_1$(a) = 1790 | | | | $\omega_1$(a) = 1763 | | | | *c* | | | |
| | $\omega_2$(a) = 466 | | | | $\omega_2$(a) = 459 | | | | *c* | | | |
| | $\omega_3$(a) = 344 | | | | $\omega_3$(a) = 379 | | | | *c* | | | |
| | $\omega_4$(a) = 225 | | | | $\omega_4$(a) = 233 | | | | *c* | | | |
| | $\omega_5$(a) = 190 | | | | $\omega_5$(a) = 181 | | | | *c* | | | |
| | $\omega_6$(a) = 160 | | | | $\omega_6$(a) = 139 | | | | *c* | | | |
| | $\omega_7$(a) = 129 | | | | $\omega_7$(a) = 100 | | | | *c* | | | |
| frequencies, $cm^{-1}$ | $\omega_8$(a) = 52 | | | | $\omega_8$(a) = 48 | | | | *c* | | | |
| | $\omega_9$(b) = 1789 | | | | $\omega_9$(b) = 1756 | | | | *c* | | | |
| | $\omega_{10}$(b) = 424 | | | | $\omega_{10}$(b) = 417 | | | | *c* | | | |
| | $\omega_{11}$(b) = 359 | | | | $\omega_{11}$(b) = 401 | | | | *c* | | | |
| | $\omega_{12}$(b) = 209 | | | | $\omega_{12}$(b) = 219 | | | | *c* | | | |
| | $\omega_{13}$(b) = 167 | | | | $\omega_{13}$(b) = 174 | | | | *c* | | | |
| | $\omega_{14}$(b) = 153 | | | | $\omega_{14}$(b) = 152 | | | | *c* | | | |
| | $\omega_{15}$(b) = 113 | | | | $\omega_{15}$(b) = 120 | | | | *c* | | | |

[a] At the CCSD(T)/6-311+G* level of theory, the total energy is −5069.725362. [b] At the MP2full/6-311+G(2df) level of theory, the total energy is −5071.777889. [c] Molecular property was not calculated at this level of theory.

(Table 4), which should correspond to a Cu−C stretching mode. The Cu−C stretch in both the linear and $C_{2v}$ isomers of $CuC_2^-$ has similar frequencies (Tables S1 and S2 in Supporting Information). Because the HOMO (13a) of $Cu_3C_4^-$ (Figure S3) represents a relatively weak bonding interaction between the $Cu_3$ unit and the $C_2$ units, the Cu−C stretching frequency in neutral $Cu_3C_4$ is not expected to change significantly from that of the anion. We note from Table 3 that the linear $Cu_3C_4^-$ isomer does not possess any symmetric modes with frequencies in the vicinity of the observed vibrational frequency for $Cu_3C_4$. Thus, the observed vibrational frequency provides additional confirmation for the sandwich isomer. In Table 6, we also presented VDEs for saddle-point structures II and III of $Cu_3C_4^-$. One can see that the ab initio photoelectron spectra for these two structures show very similar VDEs to that of structure I. Thus, the internal rotation of the $C_2^{2-}$ groups in the $Cu_3C_4^-$ sandwich should result in a contribution to the experimental spectrum from the continuum structures, but because their spectral pattern is the same, the internal rotation does not make the experimental peaks very broad.

The comparison between the theoretical results and the experimental data confirmed unequivocally that the sandwich isomer was the global minimum for $Cu_3C_4^-$. Therefore, we demonstrated that the B3LYP levels of theory overestimated

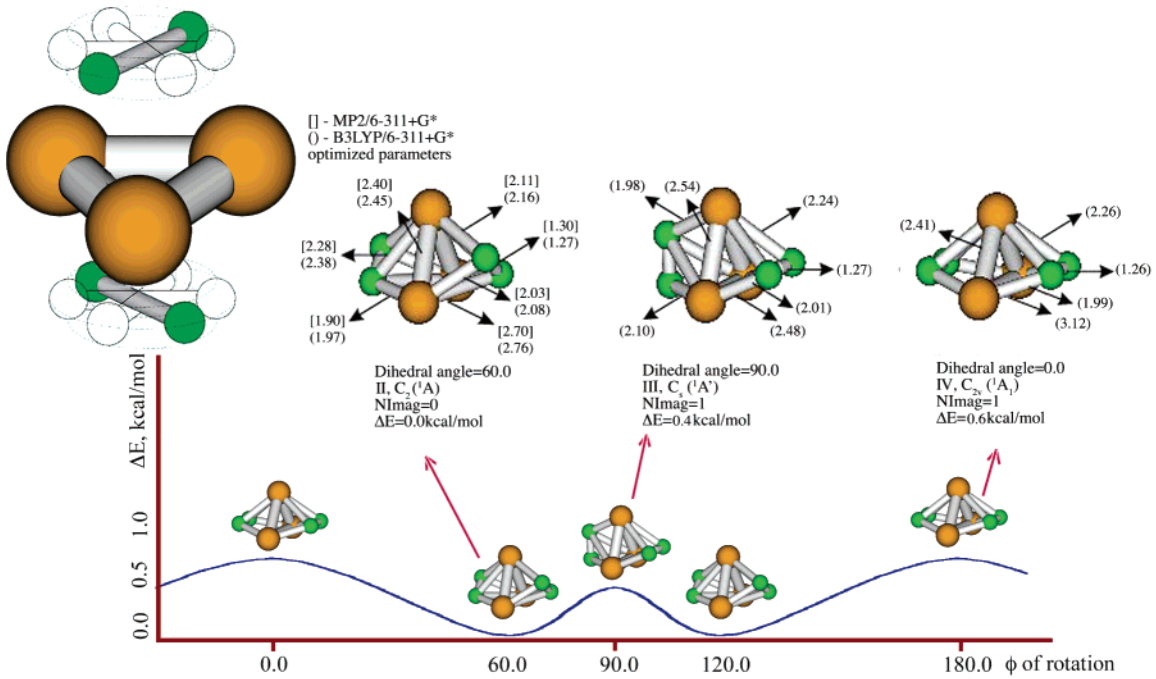


**Figure 6.** Energy diagram of the intramolecular rearrangement of the sandwich-type $Cu_3C_4^-$ structure.

**TABLE 5. Electronic Transitions of the Two Lowest-Energy Isomers of $CuC_2^-$**

| experimental spectrum | | structure I ($C_{\infty}$v, $^1\Sigma^+$) | | | structure II ($C_{2v}$, $^1$A$_1$) | | |
|---|---|---|---|---|---|---|---|
| observed feature | VDE (eV) | molecular orbital | CCSD(T)/6-311+G(2df) | TD B3LYP/6-311+G(2df) | molecular orbital | CCSD(T)/6-311+G(2df) | TD B3LYP/6-311+G(2df) |
| X[a] | 2.26(3) | | | | 5a$_1$ | 2.14 | 2.28 |
| A | 2.8−3.4 | 4$\sigma$ | 2.51 | 2.74 | 2b$_1$ | 2.92 | 2.63 |
| | | 2$\pi$ | 2.69 | 2.76 | | | |
| B | 3.88(5) | 3$\sigma$ | | 3.74 | | | |
| C | 4.22(5) | | | | 2b$_2$ | 4.36 | 4.11 |
| D | 4.63(2) | | | | | | |
| | | | | | 4a$_1$ | | 5.39 |

[a] Numbers in parentheses represent the experimental uncertainties in the last digits.

**TABLE 6. Experimental and Calculated Electronic Transitions of the Lowest-Energy Isomers of $Cu_3C_4^-$**

| experimental spectrum | | structure II ($C_2$, $^1$A) | | structure III ($C_{2v}$, $^1$A$_1$) | | structure IV ($C_s$, $^1$A′) | | structure I ($D_{\infty}$h, $^1\Sigma_g^+$) | |
|---|---|---|---|---|---|---|---|---|---|
| observed feature | VDE (eV) | molecular orbital | theor.[a] VDE (eV) | molecular orbital | theor.[a] VDE (eV) | molecular orbital | theor.[a] VDE (eV) | molecular orbital | theor.[a] VDE (eV) |
| X | 3.07(2) | 13a | 3.03 | 7b$_1$ | 2.97 | 15a′ | 3.03 | 3$\pi_g$ | 3.01 |
| A | 3.73(3) | 12b | 3.81 | 9a$_1$ | 3.68 | 14a′ | 3.85 | 5$\sigma_g$ | 3.32 |
| B | 3.97(3) | 11b | 4.17 | 6b$_1$ | 3.88 | 13a′ | 3.91 | 2$\pi_u$ | 4.08 |
| C | 4.32(2) | 12a | 4.35 | 5b$_1$ | 4.16 | 9a″ | 4.16 | 2$\pi_g$ | 4.65 |
| D | 4.58(3) | 10b | 4.60 | 8a$_1$ | 4.27 | 8a″ | 4.34 | 4$\sigma_u$ | 5.01 |
| E | 4.87(3) | 11a | 4.80 | 4a$_2$ | 4.47 | 12a′ | 4.69 | 4$\sigma_g$ | 5.12 |
| | | 10a | 4.91 | 5b$_2$ | 4.86 | 7a″ | 4.78 | 2$\pi_g$ | 6.01 |
| F | 5.16(3) | 9b | 5.12 | 4b$_2$ | 4.96 | 11a′ | 4.88 | 3$\sigma_u$ | 6.33 |
| | | 8b | 5.17 | 7a$_1$ | 5.01 | 6a″ | 5.18 | | |
| G | 5.35(3) | 9a | 5.26 | 3a$_2$ | 5.09 | 5a″ | 5.21 | | |
| | | 8a | 5.28 | 4b$_1$ | 5.32 | 4a″ | 5.23 | | |
| H | 5.46(3) | 7b | 5.44 | 6a$_1$ | 5.33 | 10a′ | 5.29 | | |
| I | 5.80(3) | 7a | 5.59 | 3b$_2$ | 5.41 | 9a′ | 5.32 | | |
| J | 5.94(3) | 6b | 5.82 | 2a$_2$ | 5.47 | 3a″ | 5.61 | | |
| K | 6.08(3) | 6a | 6.09 | 5a$_1$ | 5.76 | 8a′ | 5.94 | | |
| L | 6.20(3) | 5b | 6.67 | 3b$_1$ | 6.13 | 7a′ | 6.03 | | |
| | | 5a | 6.67 | 2b$_2$ | 6.16 | 2a″ | 6.35 | | |

[a] At the TD B3LYP/6-311+G(2df) level of theory. [b] Numbers in parentheses represent the experimental uncertainties in the last digits.

the stability of the linear isomer, whereas the MP2 and CCSD(T) results are more reliable for $Cu_3C_4^-$. The MP2 results showed that the sandwich isomer is more stable than the linear one by 12.8 kcal/mol, and a 16.0 kcal/mol energy difference was found at the CCSD(T)/6-311+G* level, explaining why the linear isomer was not observed.

### 7. Chemical Bonding in the Sandwich $Cu_3C_4^-$

The sandwich $Cu_3C_4^-$ is an interesting cluster. It may be viewed as two $C_2^{2-}$ units interacting with a triangular $Cu_3^{3+}$ unit in a strict ionic description. The fact that the $C_2$ units can almost freely rotate around the $Cu_3$ fragment is consistent with the dominantly ionic bonding character. Calculated NPA effective atomic charges at the B3LYP/6-311+G* level were found to be $Q(Cu_1) = +0.73|e|$, $Q(Cu_{2,3}) = +0.72|e|$, $Q(C_{4,5}) = -0.83|e|$, and $Q(C_{6,7}) = -0.76|e|$ in the sandwich isomer.

This agrees with the smaller $CuC_2^-$ cluster, for which there is also no strong directional preference between the $C_2$ unit and Cu. Indeed, according to the NPA calculations, the chemical bonding in both isomers of $CuC_2^-$ is quite ionic with $Q(Cu) = +0.49|e|$ and $Q(C) = -0.75|e|$ in the triangular isomer and $Q(Cu) = +0.32|e|$, $Q(C_1) = -0.92|e|$, and $Q(C_2) = -0.40|e|$ in the linear isomer. Previously, Lo et al. observed that an acetylenic $C_2$ unit is oscillating inside a $Cu_4$ rectangle and studied the $C_2$ fluxionality in solution with NMR. It would be very interesting to perform high-resolution optical spectroscopy on $Cu_3C_4^-$, which may allow the internal rotation of the $C_2$ units to be probed directly.

We also calculated nucleus-independent chemical shifts (NICS)[80] at the centrum and above the $Cu_3$ fragment. The NICS values (at B3LYP/6-311+G*) were found to be negative (−7.1 ppm at the centrum ($z = 0$), −7.9 ppm at $z = 0.4$ Å, and −17.0 ppm at $z = 0.8$ Å) showing the presence of aromaticity in the $Cu_3$ group.

### 8. Conclusions

We conducted a combined photoelectron spectroscopy and ab initio study on two copper carbide clusters in the gas phase: $CuC_2^-$ and $Cu_3C_4^-$. The clusters were generated in a laser vaporization cluster source, and $Cu_3C_4^-$ was shown to exhibit enhanced stability. PES spectra were obtained at three photon energies (355, 266, and 193 nm), and numerous well-resolved bands were observed. Significant photofragmentation was observed for $CuC_2^-$ (to $Cu^- + C_2$) during the photodetachment experiment. Extensive ab initio calculations were carried out in search of the global minimum structures. Several theoretical methods were used for $CuC_2^-$, which was used as a test case for the more complicated $Cu_3C_4^-$. Two nearly degenerate isomers were found for $CuC_2^-$, a linear $CuCC^-$ and a triangular structure, which were both observed experimentally. For $Cu_3C_4^-$, we also identified two low-lying isomers: a sandwich structure containing a $Cu_3^{3+}$ triangular group and two $C_2^{2-}$ units and a linear structure in which two $C_2$ units were separated by the Cu atoms. Comparison between the ab initio PES spectra from TD-DFT and the experimental data revealed that the sandwich $Cu_3C_4^-$ is solely responsible for the experimental spectra, and the linear isomer was not observed, suggesting that the former is the global minimum in agreement with the CCSD(T)/6-311+G* predictions. More interestingly, we found that in the sandwich $Cu_3C_4^-$ cluster there exists a relatively low barrier (0.4−0.6 kcal/mol) for the internal rotation of the $C_2^{2-}$ units, suggesting the ionic bonding nature between the $Cu_3$ unit and the $C_2$ fragments. This internal rotation may be directly probed by high-resolution optical spectroscopy.

**Acknowledgment.** The theoretical work done at Utah State University was supported by the donors of the Petroleum Research Fund (ACS-PRF no. 38242-AC6), administered by the American Chemical Society. The experimental work done at Washington State University was supported by the National Science Foundation (DMR-0095828) and performed at the W. R. Wiley Environmental Molecular Sciences Laboratory, a national scientific user facility sponsored by DOE's Office of Biological and Environmental Research and located at Pacific Northwest National Laboratory, which is operated for DOE by Battelle.

**Supporting Information Available:** Calculated molecular properties of the linear ($C_{\infty v}$, $^1\Sigma^+$) and triangular ($C_{2v}$, $^1A_1$) isomers of $CuC_2^-$ and molecular orbitals of the linear and triangular isomers of $CuC_2^-$ and the sandwich isomer of $Cu_3C_4^-$. This material is available free of charge via the Internet at http://pubs.acs.org.

### References and Notes

(1) Wells, A. F. *Structural Inorganic Chemistry*, 5th ed.; Oxford University Press: Oxford, U.K., 1984.
(2) Greenwood, N. N.; Earnshaw, A. *Chemistry of the Elements*, 2nd ed.; Butterworth-Heinemann: Oxford, U.K., 1997.
(3) Cottrell, A. *Chemical Bonding in Transition Metal Carbides*; Institute of Materials: London, 1995.
(4) Neudeck, P. G.; Matus, L. G. *An Overview of Silicon Carbide Device Technology*: National Aeronautics and Space Administration: Springfield, VA, 1992.
(5) Fuentealba, P.; Savin, A. *J. Phys. Chem. A* **2000**, *104*, 10882.
(6) Heaven, M. W.; Stewart, G. M.; Buntine, M. A.; Metha, G. F. *J. Phys. Chem. A* **2000**, *104*, 3308−3316.
(7) Rintelman, J. M.; Gordon, M. S. *J. Chem. Phys.* **2001**, *115*, 1795.
(8) Roszak, S.; Balasubramanian, K. *J. Chem. Phys.* **1997**, *106*, 4008.
(9) Roszak, S.; Balasubramanian, K. *J. Chem. Phys.* **1997**, *106*, 158.
(10) Froudakis, G.; Zdetsis, A.; Mühlhäuser, M.; Engels, B.; Peyerimhoff, S. D. *J. Chem. Phys.* **1994**, *101*, 6790.
(11) Boldyrev, A. I.; Simons, J. *J. Phys. Chem. A* **1997**, *101*, 2215.
(12) Yang D.-S.; Zgierski, M. Z.; Berces, A.; Hackett, P. A.; Roy, P.-N; Martinez, A.; Carrington, T., Jr.; Salahub, D. R.; Fournier, R.; Pang, T.; Chen, C. *J. Chem. Phys.* **1996**, *105*, 10663.
(13) Cannon, N. A.; Boldyrev, A. I.; Li, X.; Wang, L. S. *J. Chem. Phys.* **2000**, *113*, 2671.
(14) Zhai, H. J.; Wang, L. S.; Jena, P.; Gutsev, G. L.; Bauschlicher, C. W., Jr. *J. Chem. Phys.* **2004**, *120*, 8996.
(15) Zhai, H. J.; Liu, S.; Li, X.; Wang, L. S. *J. Chem. Phys.* **2001**, *115*, 5170.
(16) Li, X.; Wang, L. S. *J. Chem. Phys.* **1999**, *111*, 8389.
(17) Wang, X. B.; Ding, C. F.; Wang, L. S. *J. Phys. Chem. A* **1997**, *101*, 7699.
(18) Li, S.; Wu, H.; Wang, L. S. *J. Am. Chem. Soc.* **1997**, *119*, 22, 7417.
(19) Wang, L. S.; Cheng, H. *Phys. Rev. Lett.* **1997**, *78*, 15, 2983.
(20) Wang, L. S.; Li, S.; Wu, H. *J. Phys. Chem.* **1996**, *100*, 19211.
(21) Wang, L. S.; Wang, X. B.; Wu, H.; Cheng, H. *J. Am. Chem. Soc.* **1998**, *120*, 6556.
(22) Li, X.; Wang, L. S.; Cannon, N. A.; Boldyrev, A. I. *J. Chem. Phys.* **2002**, *116*, 1330.
(23) McElvany, S. W.; Cassady, C. J. *J. Phys. Chem.* **1990**, *94*, 2057.
(24) Chupka, W. A.; Berkowitz, J.; Giese, C. F.; Inghram, M. G. *J. Phys. Chem.* **1958**, *62*, 611.
(25) Kohl, F. J.; Stearns, C. A. *J. Phys. Chem.* **1970**, *74*, 2714.
(26) Kohl, F. J.; Stearns, C. A. *High Temp. Sci.* **1974**, *6*, 284.
(27) Gupta, S. K.; Kingcade, J. E., Jr.; Gingerich, K. A. *Adv. Mass. Spectrosc.* **1980**, *8*, 445.
(28) Guo, B. C.; Kerns, K. P.; Castleman, A. W., Jr. *Science* **1992**, *255*, 1411.
(29) Guo, B. C.; Wei, S.; Purnell, J.; Buzza, S.; Castleman, A. W., Jr. *Science* **1992**, *256*, 515.
(30) Pilgrim, J. S.; Duncan, M. D. *J. Am. Chem. Soc.* **1993**, *115*, 6958.
(31) Byun, Y. G.; Freiser, B. S. *J. Am. Chem. Soc.* **1996**, *118*, 3681.
(32) Lee, S.; Gotts, N. G.; von Helden, G.; Bowers, M. T. *Science* **1995**, *267*, 999.
(33) Dance, I. *J. Chem. Soc., Chem. Commun.* **1992**, 1779.
(34) Rohmer, M. M.; Benard, M.; Poblet, J. M. *Chem. Rev.* **2000**, *100*, 495.
(35) Yamada Y.; Castleman, A. W., Jr. *Chem. Phys. Lett.* **1993**, *204*, 133.
(36) Dance, I. *J. Am. Chem. Soc.* **1993**, *115*, 11052.
(37) Lo, W. Y.; Lam, C.-H.; Fung, W. K.-M.; Sun, H.-Z.; Yam, V. W.-W.; Balcells, D.; Maseras, F.; Eisenstein, O. *Chem. Commun.* **2003**, 1260.
(38) Vega, A.; Calvo, V.; Spodine, E.; Zarate, A.; Fuenzalida, V.; Saillard, J.-Y. *Inorg. Chem.* **2002**, *41*, 3389.
(39) Cage, B.; Cotton, F. A.; Dalal, N. S.; Hillard, E. A.; Rakvin, B.; Ramsey, C. M. *J. Am. Chem. Soc.* **2003**, *125*, 5270.

(40) Tsipis, A. C.; Tsipis, C. A. *J. Am. Chem. Soc.* **2003**, *125*, 1136.
(41) Boca, R.; Dlhan, L.; Mezei, G.; Ortiz-Perez, T.; Raptis, R. G.; Telser, J. *Inorg. Chem.* **2003**, *42*, 5801.
(42) Yam, V. W.-W.; Fung, W. K.-M.; Cheung, K.-K. *Organometallics* **1998**, *17*, 3293.
(43) Niemeyer, M. *Organometallics* **1998**, *17*, 4649.
(44) Knotter, D. M.; Grove, D. M.; Smeets, W. J. J.; Spek, A. L.; Van Koten, G. *J. Am. Chem. Soc.* **1992**, *114*, 3400.
(45) Olmstead, M. M.; Power, P. P. *J. Am. Chem. Soc.* **1990**, *112*, 8008.
(46) Kettle, S. F. A.; Bocccaleri, E.; Diana, E.; Rossetti, R.; Stanghelline, P. L.; Lapalicci, M. C.; Longoni, G. *Inorg. Chem.* **2003**, *42*, 6314.
(47) Ni, B.; Kramer, J.; Werstiuk, N. H. *J. Phys. Chem. A* **2003**, *107*, 8949.
(48) Ni, B.; Kramer, J.; Werstiuk, N. H. *J. Phys. Chem. A* **2003**, *107*, 2890.
(49) Rasika Dias, H. V.; Diyabalanage, H. V. K.; Rawashdeh-Omary, M. A.; Franzman, W. A.; Omary, M. A. *J. Am. Chem. Soc.* **2003**, *125*, 12072.
(50) Wang, X.-S.; Zhao, H.; Qu, Z.-R.; Ye, Q.; Zhang, J.; Xiong, R.-G.; You, X.-Z.; Fun, H.-K. *Inorg. Chem.* **2003**, *42*, 5786.
(51) Eriksson, H.; Ortendahl, M.; Hakansson, M. *Organometallics* **1996**, *15*, 4823.
(52) Yam, V. W.-W.; Li, W.-K.; Lai, T.-F.*Organometallics* **1993**, *12*, 2383.
(53) Eriksson, H.; Hakansson, M. *Organometallics* **1997**, *16*, 4243.
(54) Wang, L. S.; Cheng, H. S.; Fan, J. *J. Chem. Phys.* **1995**, *102*, 9480. Wang, L. S.; Wu, H. In *Advances in Metal and Semiconductor Clusters. IV. Cluster Materials*; Duncan, M. A., Ed.; JAI Press: Greenwich, CT, 1998; p 299.
(55) Parr R. G.; Yang, W. *Density-Functional Theory of Atoms and Molecules*; Oxford University Press: Oxford, U.K., 1989.
(56) Becke, A. D. *J. Chem. Phys.* **1993**, *98*, 5648.
(57) Perdew, J. P.; Chevary, J. A.; Vosko, S. H.; Jackson, K. A.; Pederson, M. R.; Singh, D. J.; Fiolhais, C. *Phys. Rev. B* **1992**, *46*, 6671.
(58) McLean A. D.; Chandler, G. S. *J. Chem. Phys.* **1980**, *72*, 5639.
(59) Clark, T.; Chandrasekhar, J.; Spitznagel, G. W.; Schleyer, P. v. R. *J. Comput. Chem.* **1983**, *4*, 294.
(60) Frisch, M. J.; Pople, J. A.; Binkley, J. S. *J. Chem. Phys.* **1984**, *80*, 3265.
(61) Cizek, J. *Adv. Chem. Phys*. **1969**, *14*, 35.
(62) Purvis, G. D., III; Bartlett, R. J. *J. Chem. Phys*. **1982**, *76*, 1910.
(63) Scuseria, G. E.; Janssen, C. L.; Schaefer, H. F., III. *J. Chem. Phys*. **1988**, *89*, 7282.
(64) Hay, P. J.; Wadt, W. R. *J. Chem. Phys.* **1985**, *82*, 270.
(65) Wadt, W. R.; Hay, P. J. *J. Chem. Phys*. **1985**, *82*, 284.
(66) Hay, P. J.; Wadt, W. R. *J. Chem. Phys.* **1985**, *82*, 299.
(67) Head-Gordon, M.; Pople, J. A.; Frisch, M. J. *Chem. Phys. Lett.* **1988**, *153*, 503.
(68) Frisch, M. J.; Head-Gordon, M.; Pople, J. A. *Chem. Phys. Lett.* **1990**, *166*, 275.
(69) Frisch, M. J.; Head-Gordon, M.; Pople, J. A. *Chem. Phys. Lett.* **1990**, *166*, 281.
(70) Bauernshmitt, R.; Alrichs, R. *Chem. Phys. Lett.* **1996**, *256*, 454.
(71) Casida, M. E.; Jamorski, C.; Casida, K. C.; Salahub, D. R. *J. Chem. Phys*. **1998**, *108*, 4439.
(72) Glendening, E. D.; Reed, A. E.; Carpenter, J. E.; Weinhold, F. *NPA*, version 3.1, 1998.
(73) Frisch, M. J.; Trucks, G. W.; Schlegel, H. B.; Scuseria, G. E.; Robb, M. A.; Cheeseman, J. R.; Zakrzewski, V. G.; Montgomery, J. A., Jr.; Stratmann, R. E.; Burant, J. C.; Dapprich, S.; Millam, J. M.; Daniels, A. D.; Kudin, K. N.; Strain, M. C.; Farkas, O.; Tomasi, J.; Barone, V.; Cossi, M.; Cammi, R.; Mennucci, B.; Pomelli, C.; Adamo, C.; Clifford, S.; Ochterski, J.; Petersson, G. A.; Ayala, P. Y.; Cui, Q.; Morokuma, K.; Malick, D. K.; Rabuck, A. D.; Raghavachari, K.; Foresman, J. B.; Cioslowski, J.; Ortiz, J. V.; Stefanov, B. B.; Liu, G.; Liashenko, A.; Piskorz, P.; Komaromi, I.; Gomperts, R.; Martin, R. L.; Fox, D. J.; Keith, T.; Al-Laham, M. A.; Peng, C. Y.; Nanayakkara, A.; Gonzalez, C.; Challacombe, M.; Gill, P. M. W.; Johnson, B. G.; Chen, W.; Wong, M. W.; Andres, J. L.; Head-Gordon, M.; Replogle, E. S.; Pople, J. A. *Gaussian 98*, revision A.7; Gaussian, Inc.: Pittsburgh, PA, 1998.
(74) Frisch, M. J.; Trucks, G. W.; Schlegel, H. B.; Scuseria, G. E.; Robb, M. A.; Cheeseman, J. R.; Montgomery, J. A., Jr.; Vreven, T.; Kudin, K. N.; Burant, J. C.; Millam, J. M.; Iyengar, S. S.; Tomasi, J.; Barone, V.; Mennucci, B.; Cossi, M.; Scalmani, G.; Rega, N.; Petersson, G. A.; Nakatsuji, H.; Hada, M.; Ehara, M.; Toyota, K.; Fukuda, R.; Hasegawa, J.; Ishida, M.; Nakajima, T.; Honda, Y.; Kitao, O.; Nakai, H.; Klene, M.; Li, X.; Knox, J. E.; Hratchian, H. P.; Cross, J. B.; Adamo, C.; Jaramillo, J.; Gomperts, R.; Stratmann, R. E.; Yazyev, O.; Austin, A. J.; Cammi, R.; Pomelli, C.; Ochterski, J. W.; Ayala, P. Y.; Morokuma, K.; Voth, G. A.; Salvador, P.; Dannenberg, J. J.; Zakrzewski, V. G.; Dapprich, S.; Daniels, A. D.; Strain, M. C.; Farkas, O.; Malick, D. K.; Rabuck, A. D.; Raghavachari, K.; Foresman, J. B.; Ortiz, J. V.; Cui, Q.; Baboul, A. G.; Clifford, S.; Cioslowski, J.; Stefanov, B. B.; Liu, G.; Liashenko, A.; Piskorz, P.; Komaromi, I.; Martin, R. L.; Fox, D. J.; Keith, T.; Al-Laham, M. A.; Peng, C. Y.; Nanayakkara, A.; Challacombe, M.; Gill, P. M. W.; Johnson, B.; Chen, W.; Wong, M. W.; Gonzalez, C.; Pople, J. A. *Gaussian 03*, revision A.1; Gaussian, Inc.: Pittsburgh, PA, 2003.
(75) Chaftenaar, G. *MOLDEN3.4*; CAOS/CAMM Center: The Netherlands, 1998.
(76) Wu, H.; Desai, S. R.; Wang, L. S. *J. Phys. Chem. A* **1997**, *101*, 2103.
(77) Ervin, K. M.; Lineberger, W. C. *J. Phys. Chem*. **1991**, *95*, 1167.
(78) Arnold, W. D.; Bradforth, S. E.; Kitsopoulos, T. N.; Neumark, D. M. *J. Chem. Phys*. **1991**, *95*, 8753.
(79) Ho, J.; Ervin, K. M.; Lineberger, W. C. *J. Chem. Phys*. **1990**, *93*, 6987.
(80) Schleyer, P. v. R.; Maerker, C.; Dransfeld, A.; Jiao, H.; Hommes, N. J. R. v. E. *J. Am. Chem. Soc.* **1996**, *118*, 6317.